DALTON
FULL PAPER

Periodic trends in the diatomic monoxides and monosulfides of the 3d transition metals

Adam J. Bridgeman * and Joanne Rothery

University Chemical Laboratories, Lensfield Road, Cambridge, UK CB2 1EW.
E-mail: ajb32@cam.ac.uk

Received 11th August 1999, Accepted 17th November 1999

Non-local, density functional calculations have been performed on the ground and low-lying excited states of the 3d transition metal monoxide and monosulfide molecules. Periodic trends in properties such as bond lengths, bond energies, vibrational force constants and dipole moments are examined. The variations in the bond lengths and energies are compared to those in the monoxide and monosulfide solids. Analysis of the electronic structures of the molecules reveals the d-orbital splitting to be $d_\pi > d_\sigma \geq d_\delta$ and shows the non-bonding role of the d_σ and d_δ functions. This sequence mirrors that in the electronically related dichloride molecules and leads to similarities in the periodic trends with those in the solids. Systematic errors in the calculated bond energies and vibrational frequencies are identified. The successful use of a correctly parameterized ligand-field model is reported allowing quantitative reproduction of the 'd–d' spectra of the monoxide molecules and the prediction of band positions of unassigned transitions.

There is considerable interest in the bonding and spectroscopic properties of the diatomic monoxides of the 3d transition metals. The electronic spectra of the monoxides are extremely complicated[1] and the assignment of the ground states has been a matter of some controversy. The strength of the metal–oxygen bond in these systems leads to their importance in astrophysics, in the vapours above the solid oxides and in high temperature chemistry.

The interaction between transition metals and oxygen is of fundamental importance. The multiple bonds have varying amounts of ionic and covalent character. The open shell nature of the majority of the molecules leads to large numbers of low-lying configurations and electronic states. This also leads to considerable difficulties in the computational study of their electronic structure and bonding with results varying with the method applied.[2–10]

The importance of these molecules outlined above has led to a considerable amount of spectroscopic data being reported and this has been comprehensively reviewed by Merer.[1] The quality of this database means that these molecules also present an opportunity to study periodic trends across the 3d transition metals. The effect on the nature and strength of the bonding with the decreases in atomic and ionic radii and ionization energies, the contraction in orbital size and the increase in metal electronegativity observed in going from left to right across the row can be probed. The studies by Anderson *et al.*[6] and Piechota and Suffczyński[8] addressed some aspects of the periodic trends in these molecules and identified a number of unanswered questions on the bonding. Siegbahn[11] has discussed similar properties of the 4d transition metal monoxides.

The purpose of this work is to compare the bonding in the 3d transition metal monoxide molecules and to identify periodic trends within a consistent and reliable level of theory. The previous work on these systems has shown that a proper description of correlation effects is required. Non-local density functional (DF) methods implicitly incorporate electron correlation and have a good record when applied to systems containing transition metal atoms. Our work using DF theory on the electronically related transition metal dichloride molecules[12] has identified key aspects of the bonding interactions and on the hybridization of the metal atom, as well as assigning unexpected ground states. This paper reports non-local DF calculations on the ground and low lying excited states of the MO molecules (M = Ca–Zn).

Whilst DF methods give a good description of the ground states of open-shell molecules, they are less successful when applied to excited states. In contrast, modern ligand-field (LF) methods have an extremely strong record in the analysis of the spectroscopic and magnetic properties of high-valent transition metal complexes.[13] As outlined above, the rich electronic spectroscopy of the transition metal monoxide molecules is of considerable importance and a great deal of work has been reported on the assignment of the many band systems reported.[1] Our earlier work on the spectrum of the NiO molecule[10] and on the dichloride molecules[12] showed how a properly parameterized LF approach can be applied to compounds with highly unusual coordination numbers. The use of this method in analysing the spectra of the remaining monoxide molecules is reported in this paper.

The bonds in monosulfides are intrinsically longer and usually weaker than in monoxides. The bonding in the diatomic monosulfides of the transition metals has received much less attention than that in the isoelectronic monoxide molecules. Anderson *et al.*[6] reported a useful comparison of the bonding in monosulfides and monoxides within a semi-empirical model. Much less experimental data is available on the monosulfide molecules so that detailed comparison of properties such as bond lengths and force constants cannot be made without their theoretical determination. A DF study of the bonding in the ground states of the MS molecules (M = Ca–Zn) is presented in this work together with a detailed comparison with the monoxide systems.

Computational details

All density functional calculations were performed here using the 'DeFT' code written by St-Amant[14] in the linear combination of Gaussian-type orbitals (LCGTO) framework. All the reported calculations used the Vosko–Wilk–Nusair[15] local spin density (LSD) approximation of the correlation part of the exchange-correlation potential with non-local corrections using the Becke[16] functional for exchange and the Perdew[17] func-

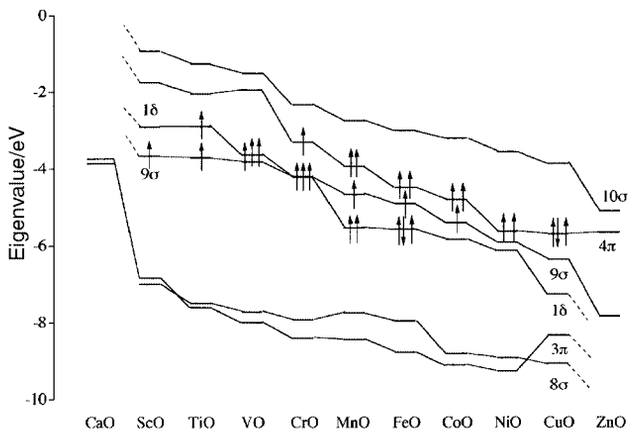

Fig. 1 Molecular orbitals for the ground states of the transition metal monoxides. The orbital occupations are shown for the half-filled orbitals with the lower levels doubly occupied.

tional for correlation. The Gaussian basis sets (GTOs) and the auxiliary basis sets needed for the Coulomb and exchange potential were optimized specifically for LSD calculations by Godbout *et al.*[18] GTO sets of double-ζ quality for the transition metals and triple-ζ quality were used for oxygen and sulfur. As single determinants are used for each state, the spin and angular momentum labels are only approximate. Bond orders were calculated from the density matrices according to the prescription suggested by Mayer.[19] The relative degree of σ- and π-charge transfer, denoted Δσ and Δπ respectively, in each state were determined from the changes in Mulliken populations compared to the fully ionic $M^{2+}O^{2-}$ formulation with the metal ion in the appropriate crystal-field configuration.

Cellular ligand-field (CLF) calculations[13] were performed with the CAMMAG4 program.[20] The parameters set consisted of e_σ and e_π(O) for the σ and π interactions between the transition metal and oxygen, the 'central' Racah parameters *B* and *C* for interelectron repulsion and ζ for spin–orbit coupling.

Results and discussion

(i) Metal monoxides

A useful starting point in describing the bonding in the monoxides is to look at the one-electron orbital energies. These are depicted in Fig. 1 for the ground states of the monoxides. The metal d-orbitals transform as $\sigma + \pi + \delta$ in the $C_{\infty v}$ point group. The molecular 1δ levels are completely non-bonding and d-orbital in character, as oxygen has no valence orbitals of δ symmetry. They fall steadily in energy across the series as the nuclear charge of the metal grows and become core-like in ZnO. The σ levels are formed from oxygen $2p_\sigma$ and metal 4s and $3d_\sigma$ functions and the π levels are formed from oxygen $2p_\pi$ and metal $3d_\pi$ functions. The oxygen 2s and the metal 4p orbitals contribute very little to the bonding.

The character of the molecular 8σ, 9σ and 10σ orbitals varies considerably in character along the period. For all the monoxides except ZnO, the 8σ level is the M–O σ-bonding orbital and is predominantly oxygen in character. The core-like nature of the zinc d-orbitals leads to this level being almost completely metal in character. In the remaining monoxides, there is considerable s–d hybridization.[10,12] This decreases the antibonding nature of the 9σ function so that it is essentially non-bonding along the series. For the early transition metals, the 4s orbital lies at lower energy than the 3d functions and the 9σ orbital is thus mostly metal 4s in character. For the later metals, the stabilization of the 3d functions results in the 9σ orbital becoming predominantly d-orbital in character. The consequences of the s–d hybridization on periodic trends such as the bond length variations are discussed below.

The 3π and 4π orbitals are the π bonding and antibonding levels respectively. At the start of the series, the 3π and 4π levels are almost completely oxygen and metal in character respectively. The increase in the electronegatively of the metal along the series leads to greater covalency in the π-bonding. The ground state of CuO has a $(4\pi)^3$ configuration with the unpaired electron residing essentially on oxygen.

These variations in the character of the valence orbitals have a number of consequences for the LF treatment of the monoxide molecules. Ligand-field theory is concerned with the spectral and magnetic properties of transition-metal complexes that arise from electronic states built from molecular functions of predominantly d-orbital character.[13] A number of the low-lying excited states of the monoxides arise from excitations involving the metal-based 1δ, 9σ and 4π levels. As outlined above, the character of the 9σ orbital varies along the series and is predominantly metal 4s in character for the early members. The 9σ–1δ and 9σ–4π transitions are then 's–d' in character and so beyond the scope of LF methods.

As shown in Fig. 1, the LF splitting in these molecules is, in general, $d_\pi > d_\sigma \geq d_\delta$. This ordering is the same as that found in other 'linear' complexes.[10,12] The ordering of d_π and d_σ is the *opposite* of that given by crystal-field or simple molecular orbital models as it implies a *smaller* σ-antibonding shift. It is now established,[10,12,13] however, that in tetragonally distorted octahedra, square-planar, linear and low-symmetry systems, the d-orbital splitting is not determined completely by the relative effectiveness of ligand σ and π donation. In these systems, the metal s- (and p-) orbitals have the same symmetry as one or more of the d-orbitals and hence mixing and stabilization of the latter can occur. The experimental or theoretical prediction of the $d_\pi > d_\sigma \geq d_\delta$ sequence does not represent a failure of LF theory, as has recently been implied.[21]

The basis of the LF approach is that the d-orbitals in high-oxidation complexes are approximately non-bonding due to their radially contracted nature. The major part of the bonding is considered to be due to the overlap of the valence orbitals of the ligands and the radially extended metal s- and p-functions. The resulting bonding and antibonding functions represent the ligand-field suffered by the d-orbitals. The energy shifts and splitting of the d-orbitals result from the interactions with these functions.[13]

In the monoxide molecules, the metal $3d_\sigma$ function interacts with four σ-functions built from the valence orbitals of the metal and oxygen ligand. These four functions derive from overlap of the oxygen 2s and $2p_\sigma$ orbitals with the metal 4s and $4p_\sigma$ orbitals. Owing to the heteropolar nature of the bonding in the monoxides, the molecular functions can be labelled according to their predominant atomic contributors as $\chi_{\sigma 1}$(O 2s), $\chi_{\sigma 2}$(O $2p_\sigma$), $\chi_{\sigma 3}$(M 4s) and $\chi_{\sigma 4}$(M $4p_\sigma$). The $3d_\sigma$ function suffers a shift due to its interaction with each part of this ligand-field. The exact energy shift of the $3d_\sigma$ orbitals is the angular overlap or CLF parameter e_σ which is given as,

$$e_\sigma = e_\sigma(\text{O 2s}) + e_\sigma(2p_\sigma) + e_\sigma(\text{M 4s}) + e_\sigma(\text{M } 4p_\sigma) \quad (1)$$

The oxygen based levels are donor functions lying at lower energy than the metal d_σ-orbital. The interactions with the metal d_σ-function are, as a result, repulsive so that the first two terms in eqn. (1) are positive. The oxygen 2s-based function is very low lying so that its energy match with the d_σ-orbital is likely to be poor. The second term is likely to dominate. The metal based levels are antibonding and empty. They are acceptor functions lying at higher energy than the d_σ-orbital so that the interactions are stabilizing. The third and fourth terms in eqn. (1) are negative. The metal $4p_\sigma$-function is very high lying so that the magnitude of the third term is likely to be far larger than the fourth term. The relative magnitudes of the dominant second and third terms are more difficult to estimate. The overall value of e_σ,

Table 1 Calculated and observed[1,22,23] properties of CaO, ScO, TiO, VO and CrO

	State	Energy/cm^{-1}		r_{M-O}/pm		D_o/kJ mol^{-1}		ω_o/cm^{-1}	
		Calc.	Obs.	Calc.	Obs.	Calc.	Obs.	Calc.	Obs.
CaO	$^1\Sigma^+$	0	0	181	182	488	376	856	—
ScO	$^2\Sigma^+$	0	0	168	167	719	676	995	965
	$^2\Delta$	11480	15019	173	173	578	496	817	834
	$^2\Pi$	15250	16498	170	169	537	479	921	869
TiO	$^3\Delta$	0	0	163	162	777	668	1008	1000
	$^1\Sigma^+$	8600	5667	162	160	674	600	1019	1013
	$^3\Pi$	12000	11899	167	—	635	526	775	864
	$^3\Phi$	15020	14019	167	167	598	500	952	860
	$^3\Sigma^-$	16130	—	169	—	585	—	897	—
VO	$^4\Sigma^-$	0	0	160	159	724	621	1028	1002
	$^4\Phi$	5600	7255	164	163	652	534	959	936
	$^2\Delta$	8500	—	159	158	832	—	1065	1020
	$^4\Delta$	18440	19148	167	169	498	392	880	835
CrO	$^5\Pi$	0	0	163	162	483	425	889	885
	$^5\Sigma^+$	9090	8191	166	166	369	327	832	868
	$^5\Delta$	13060	~11800	166	—	321	~284	830	820

$$e_\sigma \approx e_\sigma(2p_\sigma) + e_\sigma(M\ 4s) \quad (2)$$

is all that can be obtained from a LF analysis and could in principle be positive or negative. The first term in eqn. (2) represents the σ-donor ability of the ligands and the second term represents the stabilization that results from s–d hybridization.

The LF energy shift of the $3d_\pi$ orbitals is similarly given by,

$$e_\pi = e_\pi(O\ 2p_\pi) + e_\pi(M\ 4p_\pi) \quad (3)$$

where the labels in parenthesis again represent approximate descriptions of the molecular functions built from the non-d valence orbitals of the metal and ligand. The two terms in eqn. (3) represent positive and negative contributions respectively to the d-orbital energy shift. The high lying nature of the metal 4p functions means that the first term will dominate so that the e_π parameter is

$$e_\pi \approx e_\pi(O\ 2p_\pi) \quad (4)$$

and will be positive.

As there are no non-d functions of δ-symmetry, the LF energy shift of the $3d_\delta$ orbitals is simply,

$$e_\delta = 0 \quad (5)$$

The orbital ordering $d_\pi > d_\sigma \geq d_\delta$ implies that $e_\pi > e_\sigma \geq e_\delta$. As outlined above, this arises naturally from a consideration of the true ligand-field suffered by the d-orbitals and does not require that the oxygen ligand is acting as a better π- than σ-donor.

(a) CaO, ScO, TiO, VO and CrO. Table 1 lists observed and calculated properties of the ground and several low-lying excited states of the 'early' monoxides; CaO, ScO, TiO, VO and CrO. Table 2 lists the calculated bond orders and charge transfers for each state. The agreement with the spectroscopically determined properties is reasonably good although the dissociation energies are systematically overestimated. There is a slight improvement on the values obtained by Piechota and Suffczyński[8] due to the more accurate treatment of non-local corrections. The bonding in CaO is rather weaker than that in the other monoxides. This is due to the high energy of the 3d orbitals for the calcium atom. As can be seen from the π-bond order and Δπ values, this leads to much less π bonding in CaO. In CaO, ScO and TiO, the σ-bonding is M 4s–O 2p in character and appears to be similar in strength along the series. The differences in the ground state electronic configurations of these systems arise from occupation of the slightly bonding 9σ and non-bonding 1δ functions. The bond lengths therefore simply decrease along the series because of the increasing nuclear charge on the metal. The bond length contraction does not result from a bonding contribution from the 1δ functions as was suggested by Merer.[1]

Table 2 Calculated bond orders and charge transfers for low-lying states of CaO, ScO, TiO, VO and CrO. The dominant configuration outside the common . . . $(8\sigma)^2(4\pi)^4$ core is also given

	State	Configuration			Bond order		Charge transfer	
		1δ	9σ	4π	σ	π	Δσ	Δπ
CaO	$^1\Sigma^+$	0	0	0	1.19	0.68	0.61	0.58
ScO	$^2\Sigma^+$	0	1	0	1.05	1.23	0.62	0.92
	$^2\Delta$	1	0	0	1.03	1.04	0.60	0.78
	$^2\Pi$	0	0	1	1.04	1.15	0.69	0.85
TiO	$^3\Delta$	1	1	0	1.02	1.25	0.65	0.88
	$^1\Sigma^+$	2	0	0	1.37	1.03	0.64	0.95
	$^3\Pi$	0	1	1	0.98	1.13	0.65	0.83
	$^3\Phi$	1	0	1	1.00	1.10	0.64	0.49
	$^3\Sigma^-$	2	0	0	0.98	1.01	0.60	0.68
VO	$^4\Sigma^-$	2	1	0	0.97	1.23	0.63	0.87
	$^4\Phi$	1	1	1	0.97	1.07	0.66	0.82
	$^2\Delta$	1	2	0	1.01	1.42	0.61	1.39
	$^4\Delta$	1	0	2	1.00	0.85	0.69	0.67
CrO	$^5\Pi$	2	1	1	0.91	1.08	0.64	0.90
	$^5\Sigma^+$	2	0	2	0.99	0.80	0.72	0.66
	$^5\Delta$	1	1	2	0.95	0.76	0.70	0.78

A number of excited states involving rearrangement of the electrons amongst the metal-based orbitals have been observed[1] for ScO and TiO. The $^2\Delta \leftarrow {}^2\Sigma^+$ and $^2\Pi \leftarrow {}^2\Sigma^+$ transitions have been assigned for ScO corresponding to $9\sigma \rightarrow 1\delta$ and $9\sigma \rightarrow 4\pi$ excitations respectively. Use of eqns. (1)–(5) makes a LF analysis of the spectrum trivial but the validity of the LF model for this system is not verifiable. As TiO has two metal-based electrons, it is a much more stringent test of the applicability of the LF model. One- and two-electron and spin-forbidden excitations have been assigned for this system. It is not possible to fit the observed spectrum with the CLF method using a single set of parameter values. Rather than being a failure of the LF approach, this indicates that these systems are beyond the scope of LF theory. This is fully consistent with the DF characterization of the metal-based molecular orbitals.

The simple shortening of the metal–oxygen bond along the series, noted above for the first three members, continues in VO which has an extra non-bonding electron. CrO is the first molecule in the series to have an electron in the antibonding 4π orbital in its ground state. The result is a significant weakening of the bonding. Thus, CrO has a longer bond length than VO

and a significantly lower dissociation energy and stretching frequency.

The 9σ, 1δ and 4π functions are all d-orbital dominated in VO and CrO. A number of excited states due to transitions amongst this set have been assigned[1] for VO. Table 3 lists the observed transition energies and those calculated with the CLF parameters are given in Table 4 for this system. In analysing the spectrum, the spin-quartet manifold was fitted first with the complete parameter set except the Racah *C* parameter. In the spin-doublet manifold, only the energy of the $^2\Sigma^+$ (G) state has been determined experimentally with respect to the ground state. The energies of the $^2\Pi$(P) and $^2\Pi$(H) states are only known with respect to the $^2\Delta$(G) state. The value of the *C* parameter was therefore adjusted to place the $^2\Sigma^+$(G) state at the correct energy. It is very close in energy to $^4\Pi$(P) and there is strong mixing between them despite the quite small spin–orbit coupling parameter for V^{2+}. The energy of the $^2\Sigma^+$(G) state allows the prediction of the position of the other spin-doublets including the $^2\Delta$(G) state. As can be seen in Table 3, there is excellent agreement for the states of both spin manifolds. Clearly, the LF model is suitable for the analysis of VO.

Table 3 Calculated and observed[1] transition energies in the LF spectrum of VO(g). The energy of the $^2\Delta$(G) state relative to the ground state is unknown and is denoted as 'a'

	Configuration			Transition energies/cm^{-1}		
State	1δ	9σ	4π	Ω	Calc.	Obs.
$^2\Pi$(H)	1	1	1	3/2	18332	a + 8127
				1/2	18280	
$^2\Pi$(P)	0	2	1	3/2	17606	a + 7208
				1/2	17287	
$^4\Delta$(F)	1	0	2	7/2	16115	—
				5/2	16073	
				3/2	16019	
				1/2	15934	
$^4\Pi$(P)	2	0	1	5/2	12829	
				3/2	12757	12606
				1/2	12714	
				−1/2	12674	
$^2\Sigma^+$(G)	2	1	0	1/2	12429	12430
$^2\Delta$(G)	1	2	0	3/2	11102	a
				5/2	10346	
$^2\Sigma^-$(G)	2	1	0	1/2	10156	
$^4\Pi$(F)	1	1	1	5/2	10018	
				3/2	9963	9899
				1/2	9734	
				−1/2	9521	
$^2\Gamma$(G)	2	1	0	9/2	8948	—
				7/2	8928	
$^4\Phi$(F)	1	1	1	9/2	7252	
				7/2	7192	7254
				5/2	7130	
				3/2	7068	
$^4\Sigma^-$(F)	2	1	0	3/2	13	
				1/2	0	0

Table 4 CLF parameter values (in cm^{-1}) for the VO, CrO, FeO, NiO and CuO molecules

	e_σ	e_π	*B*	*C*	ζ
VO	4300	10600	300	2550	200
CrO	3650	11750	—	—	200
FeO	3640	—	—	—	380
NiO	4460	7680	320	4375	450
CuO	$e_\pi - e_\sigma = 7700$		550	3200	277

The observed ligand-field spectrum of CrO is much simpler than that for VO with only the transitions within the spin-quintet manifold of the d^4 ion having been assigned. The expected $^4\Sigma^+ \leftarrow {}^4\Pi$ and $^4\Delta \leftarrow {}^4\Pi$ transitions occur at 8191 and ≈1180 cm^{-1} respectively leading to CLF parameter values of $e_\sigma = 3650$ and $e_\pi = 11750$ cm^{-1}. A typical ζ value of 200 cm^{-1} leads to a splitting of the ground state into its spin–orbit components: $^4\Pi_3$ (201 cm^{-1}), $^4\Pi_2$ (149 cm^{-1}), $^4\Pi_1$ (98 cm^{-1}), $^4\Pi_{0+}$ (51 cm^{-1}), $^4\Pi_{0-}$ (51 cm^{-1}) and $^4\Pi_{-1}$ (0 cm^{-1}).

(b) MnO, FeO, CoO, NiO, CuO and ZnO. Table 5 lists observed and calculated properties of the ground and several low-lying excited states of the 'later' monoxides; MnO, FeO, CoO, CuO and ZnO. The calculated properties of NiO have been reported previously.[10] Table 6 lists the calculated bond orders and charge transfers for each state. The agreement between the calculated and observed properties is again reasonable and the energies of the excited states are in good agreement with those deduced from spectroscopy. An exception to this is found for CoO for which the predicted ground state is at variance with that assigned experimentally. As with the earlier oxides, the dissociation energies are systematically overestimated. Also evident in the latter oxides is a variation in the bond energies which is at variance with that found experimentally. This error is not mirrored in the bond lengths. It appears that a better treatment of electron correlation is required to reproduce the bond energies more accurately.

The bond length of MnO is slightly longer than that in CrO and this is related to the increased occupation of the strongly antibonding 4π functions. Between MnO and NiO, the extra electrons occupy the non-bonding 1δ and essentially non-bonding 9σ functions. The increasing nuclear charge thus leads to shortening of the metal–oxygen bond. The increasing electronegativity of the metal is also evident in the greater ligand-to-metal charge transfer across the series. The antibonding role of the 4π electrons is clear from the lengthening of the bond that results from excitation from 1δ or 9σ into 4π. Thus, the $(4\pi)^0$ low spin $^1\Sigma^+$ state of FeO has a 3 pm shorter bond length and a 60% higher bond order than the $(4\pi)^2$ high spin $^5\Delta$ ground state.

The bond length of CuO is longer than that in NiO and this is again related to the increased occupation of the 4π orbitals.

Table 5 Calculated and observed[1,22,23] properties of MnO, FeO, CoO, CuO and ZnO

		Energy/cm^{-1}		r_{M-O}/pm		D_o/kJ mol^{-1}		ω_o/cm^{-1}	
	State	Calc.	Obs.	Calc.	Obs.	Calc.	Obs.	Calc.	Obs.
MnO	$^6\Sigma^+$	0	0	164	165	505	370	897	832
FeO	$^5\Delta$	0	0	162	162	478	403	868	871
	$^5\Sigma^+$	5600	≈3990	166	—	406	355	863	~900
	$^5\Pi$	8170	—	167	—	375	—	833	—
	$^1\Sigma^+$	13520	—	159	—	310	—	920	—
CoO	$^4\Sigma^+$	0	—	162		526	—	867	—
	$^4\Delta$	3500	0	168	163	480	380	940	852
CuO	$^2\Pi$	0	0	173	173	300	263	662	631
	$^2\Sigma^+$	8670	7865	168	—	192	169	739	680
	$^4\Delta$	18000	15665	178	—	82	76	582	—
ZnO	$^1\Sigma^+$	0	0	171	180	152	174	720	—

Table 6 Calculated bond orders and charge transfers for low-lying states of MnO, FeO, CoO, NiO, CuO and ZnO. The dominant configurations outside the common . . . $(8\sigma)^2(3\pi)^4$ core are also given for each state

		Configuration			Bond order		Charge transfer	
	State	1δ	9σ	4π	σ	π	Δσ	Δπ
MnO	$^6\Sigma^+$	2	1	2	0.92	0.76	0.71	0.75
FeO	$^5\Delta$	3	1	2	0.85	0.70	0.66	0.85
	$^5\Sigma^+$	2	2	2	0.85	0.69	0.55	1.01
	$^5\Pi$	2	1	3	0.85	0.72	0.77	0.68
	$^1\Sigma^+$	4	2	0	0.97	1.53	0.50	1.38
CoO	$^4\Sigma^-$	4	1	2	0.87	0.59	0.68	0.91
	$^4\Delta$	3	2	2	0.86	0.58	0.45	1.13
NiO	$^3\Sigma^-$	4	2	2	0.73	0.65	0.44	1.14
	$^3\Pi$	4	1	3	0.81	0.56	0.70	0.78
	$^3\Phi$	3	2	3	0.90	0.41	0.57	0.95
CuO	$^2\Pi$	4	2	3	0.84	0.34	0.53	0.97
	$^2\Sigma^+$	4	1	4	0.73	0.57	1.08	0.31
	$^2\Delta$	3	2	4	0.85	0.71	1.32	0.12
ZnO	$^1\Sigma^+$	4	2	4	0.83	0.49	0.98	0.36

The low energy of the 3d orbitals in this part of the series is apparent in the position of the 1δ functions in Fig. 1. In NiO, the metal : oxygen composition of the 4π orbitals is approximately 60 : 40. In CuO, this ratio is reversed. In ZnO, the 3d-orbitals are essentially core-like. The 4π orbitals are dominated by the oxygen $2p_\pi$ functions and are slightly bonding with the metal $4p_\pi$ orbitals. The result is a slightly higher π-contribution to the bond and a shorter bond length.

As outlined above, the predicted $^4\Sigma^-$ ground state of CoO does not appear to agree with the $^4\Delta$ ground state deduced experimentally.[1] The gas-phase infrared spectrum of CoO was assigned by DeVore and Gallaher[24] with a $^4\Sigma^-$ ground state. A matrix study by Green *et al.*[25] was also found to be consistent with this. However, the absence of an EPR spectrum in the matrix study by Van Lee *et al.*[26] was interpreted to indicate an orbitally degenerate $^4\Delta$ ground state. Rotational analysis of electronic bands in a laser fluorescence study by Adam *et al.*[27] strongly suggested a $^4\Delta$ ground state. The theoretical studies by Krauss and Stevens,[2] Langhoff and Bauschlicher[7] and Piechota and Suffczyński[8] predicted $^4\Sigma^-$ ground states whilst Dolg *et al.*[4] found the $^4\Delta$ state to be lower.

The required error in the relative energies of the $^4\Sigma^-$ and $^4\Delta$ states for the DF calculations to be incorrect is larger than that in the energies of the excited states in the other molecules in the set presented here. The calculated properties of the $^4\Sigma^-$ state are in good agreement with the spectroscopic properties of the ground state. CLF calculations using the parameters for NiO reported previously[10] and repeated in Table 4, also leads to a $^4\Sigma^-$ ground state with a 4 cm^{-1} zero-field splitting. The $^4\Delta$ state is predicted to be very close in energy with spin–orbit components: $^4\Delta_{7/2}$ (468 cm^{-1}), $^4\Delta_{5/2}$ (720 cm^{-1}), $^4\Delta_{3/2}$ (1017 cm^{-1}) and $^4\Delta_{1/2}$ (1017 cm^{-1}). The absence of an EPR spectrum may thus be due to the low energy excited levels near the ground state. The splitting of 252 cm^{-1} between the $\Omega = 7/2$ and $\Omega = 5/2$ is in excellent agreement with the gap of 240 cm^{-1} estimated from the laser fluorescence study by Adam *et al.*[27] The agreement between the vibrational frequency of the lower state in the fluorescence study and in the matrix infrared work could be due to the similar energies of the $^4\Sigma^-$ and $^4\Delta$ states. This would lead to considerable spin–orbit coupling between the two states so that the orbital labels become irrelevant.

The electronic spectrum of FeO is extremely rich and complicated. Two spin-allowed, 'd–d' transitions are expected: $^4\Sigma^+ \leftarrow {}^4\Delta$ and $^4\Pi \leftarrow {}^4\Delta$. Unfortunately, only the former has been assigned. The CLF analysis is thus based only on the energy of this transition (3990 cm^{-1}) and on the experimentally well-defined spin–orbit splitting[1] of the $^4\Delta$ ground state. Use of eqns. (1)–(4) shows that it is not possible to obtain a value for e_π from this database. Using the CLF parameters listed in Table 4, the energy of the $^4\Sigma^+ \leftarrow {}^4\Delta$ excitation is reproduced exactly. The spin–orbit splitting of the ground state leads to levels at $^4\Delta_4$ (0 cm^{-1}), $^4\Delta_3$ (185 cm^{-1}), $^4\Delta_2$ (373 cm^{-1}), $^4\Delta_1$ (563 cm^{-1}) and $^4\Delta_0$ (755 cm^{-1}), again in excellent agreement with the experimental results.

Table 7 Calculated and observed[22,23] properties for the ground states of the CaS–ZnS molecules. The $^4\Sigma^-$ state of CoS is calculated to lie 1770 cm^{-1} above the $^4\Delta$ state

		r_{M-O}/pm		D_o/kJ mol^{-1}		ω_o/cm^{-1}	
	State	Calc.	Obs.	Calc.	Obs.	Calc.	Obs.
CaS	$^1\Sigma^+$	232	232	385	338	476	238
ScS	$^2\Sigma^+$	215	214	527	473	593	388
TiS	$^3\Delta$	209	209	575	463	544	335
VS	$^4\Sigma^-$	207	210	517	444	527	322
CrS	$^5\Pi$	208	210	359	328	442	228
MnS	$^5\Sigma^+$	204	207	409	280	514	315
FeS	$^3\Delta$	200	200	380	318	544	355
CoS	$^4\Delta$	196	200	436	328	475	282
	$^4\Sigma^-$	195	—	414	—	480	—
NiS	$^3\Sigma^-$	197	200	355	338	513	322
CuS	$^2\Pi$	207	205	294	270	388	189
ZnS	$^1\Sigma^+$	208	210	140	—	412	215

Table 8 Calculated bond orders and charge transfers for the ground states of CaS–ZnS. The dominant configuration outside the common . . . $(8\sigma)^2(4\pi)^4$ core is also given

		Configuration			Bond order		Charge transfer	
	State	1δ	9σ	4π	σ	π	Δσ	Δπ
CaS	$^1\Sigma^+$	0	0	0	0.95	0.96	0.65	0.58
ScS	$^2\Sigma^+$	0	1	0	0.97	1.45	0.69	0.97
TiS	$^3\Delta$	1	1	0	0.94	1.36	0.66	0.92
VS	$^4\Sigma^-$	2	1	0	0.88	1.24	0.64	0.90
CrS	$^5\Pi$	2	1	1	0.87	1.05	0.65	1.04
MnS	$^6\Sigma^+$	2	1	2	0.97	0.91	0.81	0.85
FeS	$^5\Delta$	3	1	2	0.94	0.84	0.75	1.00
CoS	$^4\Delta$	3	2	2	0.97	0.90	0.56	1.25
	$^4\Sigma^-$	4	1	2	0.97	0.98	0.95	0.84
NiS	$^3\Sigma^-$	4	2	2	1.01	0.70	0.63	1.26
CuS	$^2\Pi$	4	2	3	1.07	0.37	0.76	1.06
ZnS	$^1\Sigma^+$	4	2	4	1.12	0.71	1.27	0.39

A CLF analysis of the spectrum of NiO has been reported previously[10] and the parameter set is reproduced in Table 4. These parameters lead to quantitative reproduction of the ligand-field spectrum within both the spin-triplet and spin-singlet manifolds. Two 'd–d' transitions are expected for the d^9 system CuO: $^2\Sigma^+ \leftarrow {}^2\Pi$ and $^2\Delta \leftarrow {}^2\Pi$. Unfortunately, only the former has been assigned. The CLF analysis is thus based only on the energy of this transition (7865 cm^{-1}) and on the experimentally well-defined spin–orbit splitting[1] of the $^2\Pi$ ground state. With this database and eqns. (1)–(4), only the relationship between e_σ and e_π can be determined. This is given in Table 4. Use of the e_σ value for NiO leads to a $^2\Delta \leftarrow {}^2\Pi$ transition energy of *ca.* 12500 cm^{-1}. The spin–orbit splitting of the ground state into $^2\Pi_{3/2}$ (0 cm^{-1}) and $^2\Pi_{1/2}$ (277 cm^{-1}) requires an unusually small value of ζ for a Cu^{2+}-containing molecule. This is directly related to the considerable covalency in CuO and the large oxygen contribution to the 4π orbitals described above.

(ii) Metal monosulfides

The orbital sequence in the monosulfides mirrors that in the monoxides with the d-orbitals split in the order $d_\pi > d_\sigma \geq d_\delta$. Table 7 lists the calculated and observed properties of the CaS–ZnS molecules. Table 8 lists the calculated bond orders and charge transfers for the ground state of each molecule. As in the

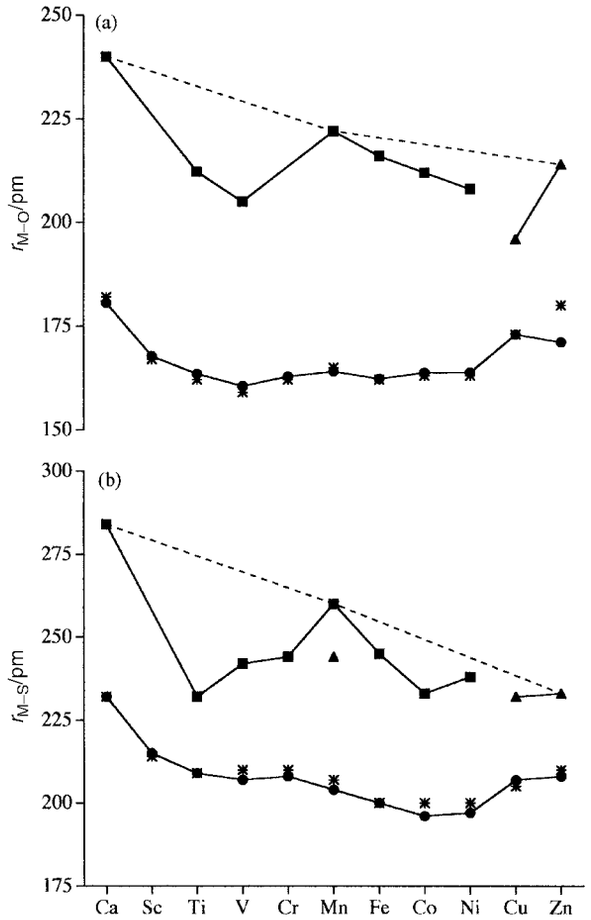

Fig. 2 Bond lengths for (a) transition metal monoxides and (b) transition metal monosulfides. Calculated (∗) and experimental (●) values for the molecules and experimental values for the 6-coordinate (■) and 4-coordinate (▲) solids are shown.

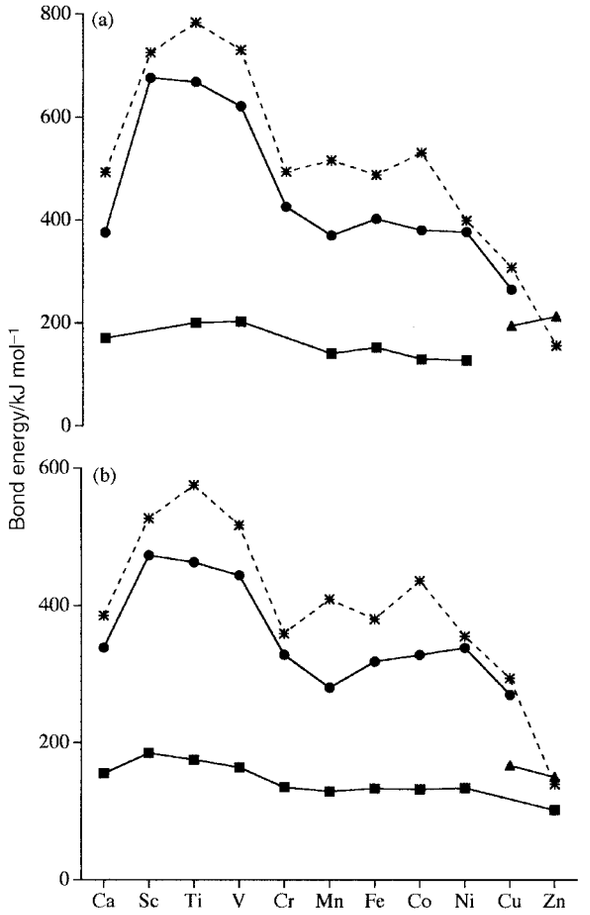

Fig. 3 Bond energies for (a) transition metal monoxides and (b) transition metal monosulfides. Calculated (∗) and experimental (●) values for the molecules and experimental values for the 6-coordinate (■) and 4-coordinate (▲) solids are shown.

monoxides, the reproduction of the experimentally determined properties is reasonable although the vibrational frequencies are all too high. As noted above for the oxides, there is also a systematic overestimation of the bond energies and the details of their variation for the sulfides of the latter elements.

The ground states are identical to those in isoelectronic monoxides except in the case of the cobalt system. As described above, the relative energy of the $^4\Sigma^-$ and $^4\Delta$ states of CoO have received considerable experimental and theoretical study with the former predicted to be the ground state in the DF calculations reported here. In CoS, however, the ground state is predicted to be $^4\Delta$, although the $^4\Sigma^-$ state is only 1770 cm^{-1} higher in energy. No detailed experimental studies of the ground state of $^4\Delta$ appear to have been reported.

The variation in the bond lengths mirrors that discussed above for the monoxides with an overall decrease across the series but with the effect of occupation of the antibonding π-levels significant in CrS and CuS. The lower electronegativity of sulfur is apparent in greater charge transfers, especially in the sulfides of the later, more electronegative metals. The values of Δπ, in particular, are significantly larger in the monosulfides than in the monoxides.

(iii) Periodic trends

Fig. 2 shows the variations in the metal–oxygen and metal–sulfur bond lengths for the monoxide and monosulfide molecules and solids.[28] Fig. 3(a) shows the variations in the metal–oxygen bond strength for the MO molecules and solids. Fig. 3(b) shows the analogous variations for the metal–sulfur bond strength. The *single* bond strengths per bond for the solids were determined, following Anderson *et al.*,[6] from the experimental lattice energies of the monoxides[29] and monosulfides[30] by dividing ΔH for the reaction,

$$MX(S) \longrightarrow M(g) + X(g) \qquad (5)$$

(where M = Ca–Zn and X = O, S) by the coordination number of the metal.

As shown in Fig. 2, the bond lengths for the monoxide and monosulfide molecules are considerably shorter than in the higher coordinate bulk species. In the molecules, there is an overall decrease in bond length across the series due to the increasing nuclear charge on the metal. This is also found in the solid species, although this is complicated slightly by changes in structure, coordination numbers and probable metal–metal bonding in the early members of the series. Superimposed on the overall contractions in the molecules and solids are 'double humps' showing the effect of the asymmetrical occupation of the d-orbitals. The dotted lines in Fig. 2 show the smooth variation for the solids when this ligand-field effect is absent and mirrors that observed in p-block and f-block compounds.

The periodicity in the bond lengths in the solids is, of course, a well-known feature in transition metal chemistry. In octahedrally coordinated complexes and compounds with π-donor ligands, the 3d-orbitals of the metal are split into *slightly* π-antibonding t_{2g} and more strongly σ-antibonding e_g orbitals. Occupation of the former between d^0 CaX(s) and d^3 VX(s) (X = O, S) causes insufficient lengthening of the bond to overcome the effect of extra nuclear charge on the metal so that there is net contraction. In high spin d^4 CrX(s) and d^5 MnX(s),

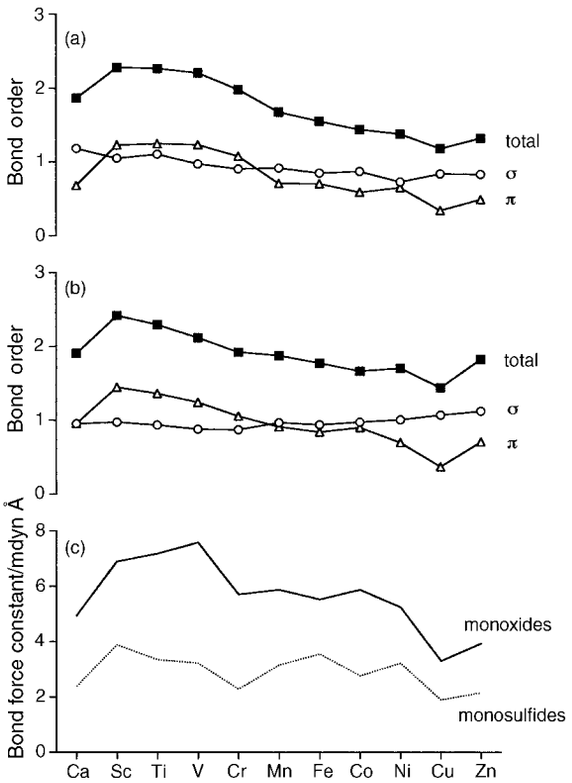

Fig. 4 (a) Bond orders for transition metal monoxides, (b) bond orders for transition metal monosulfides and (c) bond force constants.

however, the e_g orbitals are occupied and these are sufficiently antibonding to cause the bonds to lengthen *despite* the higher nuclear charges. For the d^6–d^{10} species, these trends are repeated as the orbitals become doubly occupied and a 'double hump' in the bond lengths results.

In the MX molecules, the 3d-orbitals are split into $\delta + \pi + \sigma$. As described above, the d_δ orbitals are completely non-bonding in these molecules. Hybridization between the 4s and d_σ orbitals acts to produce an approximately non-bonding σ-function which places electron density perpendicular to the M–X bond. The d_π orbitals are strongly antibonding. The resulting splitting is $d_\pi > d_\sigma \geq d_\delta$. Occupation of the d_σ and d_δ functions between d^0 CaX and d^3 VX (X = O, S) thus leads to contraction of the bond length due to the increase in nuclear charge. In high spin d^4 CrX and d^5 MnX, however, the d_π orbitals become occupied and these are sufficiently antibonding to cause the bonds to lengthen *despite* the higher nuclear charges. For the d^6–d^{10} MX molecules, these trends are repeated as the orbitals become doubly occupied and a 'double hump' in the bond lengths again results.

The bond energy variations, shown in Fig. 3, are more complicated. As expected, the bond strengths in the molecules are significantly higher than in the solids. Fig. 4 illustrates the changes in the bond orders, including the σ and π contributions, and bond force constants for the monoxide and monosulfide molecules. The graphs show that, as suggested above, the calcium systems are slightly anomalous due to the unavailability of the 3d orbitals. The bond orders show that this particularly affects the π-bonding in CaO and CaS. The σ-bonding is dominated by the overlap of the metal 4s and the ligand p_σ and the bond orders show that this is approximately constant across the two series. The bond energies and force constants in the molecules show an overall decrease across the period as the metal d-orbitals become contracted. The effect of occupying the antibonding d_π is again evident with distinct dips in the bond strengths at d^4 Cr^{2+} and d^9 Cu^{2+}. The result is 'double-hump' curves in the bond energies and force constants. The contraction of the d-orbitals across the series means that the

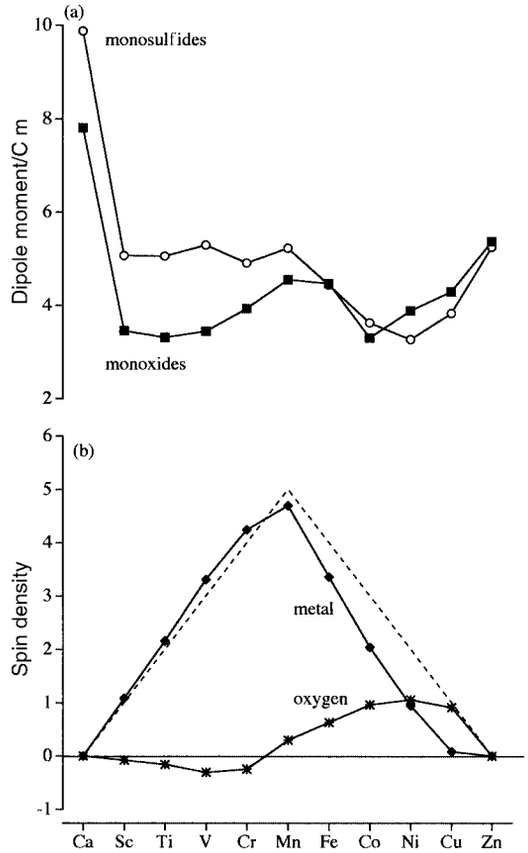

Fig. 5 (a) Dipole moments for transition metal monoxides and monosulfides and (b) spin density for the metal and oxygen atoms. A positive value indicates excess α spin and a negative value indicates excess β spin. The dotted line indicates the total excess spin in the molecule.

'hump' in the bond strengths of the first half of each series is larger than in the second half.

Fig. 5(a) shows the variations in the calculated dipole moments for the monoxide and monosulfide molecules. The dipole moments mirror the Mulliken charges listed in Tables 2, 6 and 8. The CaO and CaS molecules have much greater ionic character than the other species. This is again related to the high energy of the Ca^{2+} d-orbitals which minimizes π-donation by the ligand. Although the electronegativity of the metals increases across the series, the variation in the dipole moment is not smooth. Occupation of the d_π orbitals acts to decrease the π-donation by the ligand and so to increase the dipole moment. The dipole moments of the MS species in the first half of the series are greater than those of the MO systems. This is simply related to the longer bonds in the former as the metal charges are larger in the monoxide molecules. In the latter part of the series, the dipole moments are similar in the monoxides and monosulfides despite the longer M–S bonds.

Fig. 5(b) shows the spin density on the metal and oxygen atoms in the ground states of the MO molecules. In the early part of the series, the majority of the spin is localized on the metal. The net spin on the metal, however, exceeds the overall spin of the molecule (indicated by the dotted line on Fig. 5(b)) and there is a small minority spin density on the oxygen atom. In MnO, the majority spin is still localized on the metal but this is now less than the total spin. In CoO and NiO, there is more equal sharing of the excess spin between metal and ligand. The majority spin dominates for the oxygen atom in CuO. Piechota and Suffczyński[8] noted these trends and the antiparallel coupling in the early members of the series but were unable to provide an explanation.

In ScO, TiO and VO, the unpaired electrons occupy the 1δ and 9σ orbitals. As described above, the lack of low-lying

δ functions on the ligand and the effective s–d hybridization on the metal act to make these orbitals almost completely metal in character. As a result, the unpaired spin density resides on the metal. To minimize repulsion between the metal-based unpaired electrons and the bonding electrons, the LSD calculations lead to polarized functions for the doubly occupied levels. Thus, if the unpaired electrons in TiO are designated to be of α-spin, the 8σ α-spin orbital is 53% metal whilst the β-spin orbital is 46% metal. This polarization increases the majority spin on the metal atom and produces a minority spin on the oxygen atom. In CrO–CuO, there are unpaired electrons in the 4π orbitals. As this orbital results from the overlap of the metal $3d_\pi$ and the oxygen $2p_\pi$ functions, occupation leads to unpaired electron density on both atoms. As described above, the metal d-orbitals lower significantly in energy as the series is crossed and the 4π orbitals become increasingly dominated by the oxygen. CuO has a $(4\pi)^3$ configuration and the unpaired electron is essentially localized on the oxygen.

Concluding remarks

The lower coordination number in the 3d transition metal monoxide and monosulfide molecules leads to much shorter and stronger bonds than in the solids. In the molecules, the d-orbitals are split into three sets: σ, π and δ. Strong s–d hybridization, however, leads to stabilization of the σ-function so that it is effectively non-bonding and only the d_π functions play a strongly antibonding role. The ligand-field potential experienced by the M^{2+} results from the effects of both occupied ligand-based and unoccupied metal-based functions. The d-orbital splitting that results is $d_\pi > d_\sigma \geq d_\delta$. Proper treatment of the LF within the CLF formalism allows quantitative reproduction of the electronic spectra and the prediction of previously unassigned band positions.

The splitting of the d-orbitals thus resembles the $e_g > t_{2g}$ splitting found for octahedrally coordinated transition metal cations in the solid oxides and sulfides. This leads to greater similarity in properties such as bond lengths and strengths for the molecular and solid state species than might be expected. The "double hump" periodicity found for the properties of the solids is mirrored in that in the molecules. As the period is crossed, the molecules become more covalent and the unpaired spin density becomes less metal based. The electronic structure of the MO and MS molecules is similar although the M–S bonds are intrinsically longer and weaker. The lower electronegativity of sulfur leads to S^{2-} being a better σ- and π-donor.

The reproduction of the properties of these open-shell transition metal compounds represents a considerable challenge for theoretical techniques. The non-local density functional (DF) methods employed lead to reasonable results and allow analysis of the key variations in electronic structure. Systematic errors are revealed, however, particularly in the bond energies and vibrational frequencies of both the oxides and sulfides.

Acknowledgements

The authors would like to thank Dr Alain St-Amant of the University of Ottawa for making the DeFT code publicly available and Dr Malcolm Gerloch for use of the CAMMAG4 program. J. R. acknowledges the receipt of an EPSRC studentship and Trinity College, Cambridge for financial support.

References

1 A. J. Merer, *Ann. Rev. Phys. Chem.*, 1989, **40**, 407.
2 M. Krauss and W. J. Stevens, *J. Chem. Phys.*, 1985, **82**, 5584.
3 C. W. Bauschlicher, Jr. and S. R. Langhoff, *J. Chem. Phys.*, 1986, **85**, 5936.
4 M. Dolg, I. Wedig, H. Stoll and H. Preuss, *J. Chem. Phys.*, 1987, **86**, 2123.
5 J. M. Sennesal and J. Schamps, *Chem. Phys.*, 1987, **114**, 37.
6 A. B. Anderson, S. Y. Hong and J. L. Smialek, *J. Phys. Chem.*, 1987, **91**, 4250.
7 S. R. Langhoff and C. W. Bauschlicher, Jr., *Annu. Rev. Phys. Chem.*, 1988, **39**, 181.
8 J. Piechota and M. Suffczyński, *Phys. Rev. A*, 1993, **48**, 2679.
9 J. Piechota and M. Suffczyński, *Z. Phys. Chem.*, 1997, **200**, 39.
10 A. J. Bridgeman, *J. Chem. Soc.*, *Dalton Trans.*, 1996, 4555.
11 P. E. M. Siegbahn, *Chem. Phys. Lett.*, 1993, **201**, 15.
12 A. J. Bridgeman, *J. Chem. Soc.*, *Dalton Trans.*, 1996, 2601; A. J. Bridgeman and C. H. Bridgeman, *Chem. Phys. Lett.*, 1997, **272**, 3; A. J. Bridgeman, *J. Chem. Soc.*, *Dalton Trans.*, 1997, 4765.
13 A. J. Bridgeman and M. Gerloch, *Prog. Inorg. Chem.*, 1996, **45**, 179.
14 A. St-Amant, DeFT, a FORTRAN program, University of Ottawa, 1994.
15 S. H. Vosko, L. Wilk and M. Nusair, *Can. J. Phys.*, 1980, **58**, 1200.
16 A. D. Becke, *Phys. Rev. A*, 1988, **38**, 3098.
17 J. P. Perdew, *Phys. Rev. B*, 1986, **33**, 8822.
18 N. Godbout, D. R. Salahub, J. Andzelm and E. Wimmer, *Can. J. Chem.*, 1992, **70**, 1992.
19 I. Mayer, *Chem. Phys. Lett.*, 1983, **97**, 270; I. Mayer, *Int. J. Quantum Chem.*, 1984, **26**, 151.
20 A. R. Dale, M. J. Duer, N. D. Fenton, M. Gerloch and R. F. McMeeking, CAMMAG4, a FORTRAN program, Cambridge Univeristy, 1994.
21 S. G. Wang and W. H. E. Schwarz, *J. Chem. Phys.*, 1998, **109**, 7252.
22 G. Herzberg, *Spectra of Diatomic Molecules*, Van Nostrand-Reinhold, New York, 1950.
23 A. I. Boldyrev and J. Simons, *Periodic Table of Diatomic Molecules*, Wiley, New York, 1997.
24 T. C. DeVore and T. N. Gallaher, *J. Chem. Phys.*, 1979, **71**, 1979.
25 D. W. Green, G. T. Reedy and J. G. Kay, *J. Mol. Spectrosc.*, 1979, **78**, 257.
26 R. J. Van Lee, C. M. Brown, K. J. Zeringue and W. Weltner, *Acc. Chem. Res.*, 1980, **13**, 237.
27 A. G. Adam, Y. Azuma, J. A. Barry, G. Huang, M. P. J. Lyne, A. J. Merer and J. O. Schröder, *J. Chem. Phys.*, 1987, **86**, 2123.
28 R. W. G. Wyckoff, *Crystal Structures*, Interscience, New York, 1960; A. F. Wells, *Structural Inorganic Chemistry*, Oxford University Press, 1975.
29 *CRC Handbook of Chemistry and Physics*, ed. C. D. Hodgman, Chemical Rubber Co., Cleveland, OH, 1962.
30 K. C. Mills, *Thermodynamic Data for Inorganic Sulphides, Selenides and Tellurides*, Butterworth's, London, 1974.

Paper a906523g